COMPARISON OF EXPERIMENTAL RESPONSE SURFACE METHODOLOGY AND COMPUTATIONAL FLUID DYNAMICS STUDIES IN 6063 ALUMINIUM ALLOY THERMOSYPHON USING IRON (II, III) OXIDE NANOFLUID

[1]*DR.N.ALAGAPPAN, [2]DR.N.KARUNAKARAN

ABSTRACT--This study presents a comparison of the results obtained from experiments response surface methodology(RSM) and computational fluid dynamics (CFD) of the 6063 aluminium alloy two phase closed thermosyphon (TPCT) using Iron (II, III) oxide(Fe_3O_4) water based nano fluid. A 17 set of experimental reading were taken by response surface methodology. The input responses are heat input, angle of orientation and flow rate of water in condenser section of TPCT. The output response to be compared with RSM and CFD is thermal resistance (R_{th}). The data derived from experimental were validated by CFD using Volume of fluid (VOF) model. A reasonable good agreement was obtained between the results of the experimental RSM and CFD.

Keywords-- RSM, CFD,6063AA TPCT, Fe_3O_4 water based nano fluid

I. INTRODUCTION

TPCT is one of the promising devices and hence it is adopted for electronic cooling applications, refrigeration systems, solar energy conversion systems and waste heat recovery systems. The Two Phase Closed Thermosyphon (TPCT) is a highly effective passive device for transmitting heat at high rates. This device makes use of high heat transfer coefficients available during phase change of the working fluid. A TPCT is a gravity-assisted wickless heat pipe (Faghri, 1995). The condenser section is located above the evaporator so that the condensate is returned by gravity. The sonic and vapour pressure limits are constraints to the operation of the thermosyphon as with capillary-driven heat pipes. The entrainment limit is more profound in the thermosyphon than in capillary-driven heat pipes due to the free liquid surface. The boiling limit in TPCT occurs when a vapour film forms between the pipe wall and the liquid in the evaporator section. For small liquid fill volumes, the dry out limit may be reached, where all of the working fluid is held in the liquid film, and no liquid pool exists.

Manohar et al **(2013)** discussed the use of Box Behnken design approach to plan the experiments for turning Inconel 718 alloy with an overall objective of optimizing the process to yield higher metal removal, better surface quality and lower cutting forces. Response Surface methodology (RSM) has been adopted to express the output

---

[1] *Assistant professor, Department of Mechanical Engineering, Annamalai University, Indiaalgatesmech06@gmail.com.*

[2] *Professor, Department of Mechanical Engineering, Annamalai University, India.*

parameters (responses) that are decided by the input process parameters. Box-Behnken design is having the maximum efficiency for an experiment involving three factors and three levels; further, the number of experiments conducted for this is much lesser compared to a central composite design. The proposed Box-Behnken design requires 15 runs of experiment for data acquisition and modeling the response surface. Oguz Perincek et al **(2013)** aimed to deal with the interactions of harmonic currents produced by different single phase loads. For this purpose, compact fluorescent lamps, incandescent lamps, and electric heaters were chosen as single phase loads. The study was performed by adopting a full range of response surface methodology using Box–Behnken experimental design to express the net harmonic current (3rd and 5th) as an empirical model. The model provided an excellent explanation of the relationship among the number of loads and the net harmonic currents. Contour graphs of some of the harmonic currents was plotted to show the interactions clearly and to discuss the results of model in the graphic detail. The results of experiments showed that the harmonic interaction between the loads can be defined as a regression model which is statistically significant. Krishna et al **(2013)** investigated the the potential use of Borasus flabellifer coir powder for the removal of chromium (VI) from aqueous solution using batch mode experiments. Percentage removal of chromium (VI) is found to be 97.6% at pH 2, amount of adsorbent dosage of 0.5 g in 50 mL solution and temperature of 303 K. Influences of parameters like initial chromium (VI) concentration (5-30 mg/L), pH (1-3), and biomass dosage (10-14 g/L) on chromium (VI) adsorption were examined using response surface methodology. The Box-Behnken experimental design in response surface methodology was used for designing the experiments as well as for full response surface estimation and 15 trials as per the model were run. The optimum conditions for maximum removal of chromium (VI) from an aqueous solution of 20 mg/L were as follows: adsorbent dosage (10.1869 g/L), pH 1.9 and initial chromium (VI) concentration (6.3244 mg/L). The high correlation coefficient ($R2 = 0.989$) between the model and the experimental data showed that the model was able to predict the removal of chromium (VI) from aqueous solution using B. flabellifer coir powder efficiently. Fadhl et al **(2013)** modelled a comprehensive CFD modelling to simulate the details of the two-phase flow and heat transfer phenomena during the operation of a wickless heat pipe or thermosyphon. Water was used as the working fluid. The volume of the fluid (VOF) model in ANSYS FLUENT was used for the simulation. The evaporation, condensation and phase change processes in a thermosyphon were dealt with by adding a user-defined function (UDF) to the FLUENT code. The simulation results were compared with experimental measurements at the same condition. The simulation was successful in reproducing the heat and mass transfer processes in a thermosyphon. Good agreement was observed between CFD predicted temperature profiles and experimental temperature data. Zhi Xu et.al **(2016)** developed to simulate heat transfer characteristics and phase change process for a two-phase closed thermosyphon. The mass transfer process is implemented by adding User Define Function (UDF) to FLUENT code. The results obtained from this study show that the model with transient mass transfer time relaxation parameter has smaller relative errors (0.27–0.73%) for absolute temperature distributions along the wall of a two-phase closed thermosyphon than the model without transient mass transfer time relaxation parameter (2.01–2.97%). The model with transient mass transfer time relaxation parameter had smaller relative errors for the thermal resistances at evaporation and condensation sections (3.21–4.23% and 2.45–6.78%) than the model without transient mass transfer time relaxation parameter (18.31–21.74% and 15.34–28.25%), respectively. This study presents a comparison of the results obtained from experiments response surface methodology(RSM) and

computational fluid dynamics (CFD) of the 6063 aluminium alloy two phase closed thermosyphon (TPCT) using Iron (II,III) oxide(Fe$_3$O$_4$) water based nano fluid .

II.   IRON II, III OXIDE (FE3O4) NANOFLUID

Iron oxides are common natural compounds and can also easily be synthesized in the laboratory. There are sixteen iron oxides, including oxides, hydroxides and oxides-hydroxides. These minerals are a result of aqueous reactions under various redox and pH conditions. They have the basic composition of Fe, O and/or OH, but differ in the valency of iron and overall crystal structure (Schwertmann et al, 2008 and Cornell, Rochell)

Iron oxide nano particle consists of maghemite (γ-Fe$_2$O$_3$) and/or magnetite (Fe$_3$O$_4$) particles with diameters ranging from 1 to 100 nm (Cordova.G, 2014, and Huminic.G,2011 ,Xie.J and Jon.S, 2012). All the research studies show that the heat transfer enhancement is seen in iron oxide nano particles. Tae-Keun et al (2005) studied the effect of intrinsic thermal property of dispersed nano particles, by comparing iron (Fe) nano fluids with copper (CU) nano fluids. They found that the thermal conductivity of a Fe nano fluid increased nonlinearly upto 18 percent. Goshayeshi et al (2016) reported the aqueous Fe$_3$O$_4$ nano fluid obtained 38% of heat transfer enhancement.

2.1. Preparation of nanofluid

In the present work, two step methods were employed to prepare the nanofluids. Fe$_3$O$_4$ (iron II, III oxide) nano particles (30 nm) purchased form USA is well dispersed into DI water at a concentration of 80 mg/lit. The well dispersed sample is subjected to the sonication process in bath type ultrasonic homogenizer (Olee Pvt Ltd, 42K$_{HZ}$) up to 14 hours. To stabilize the nanofluids, few drops of kerosene along with oleic acid of (C$_{18}$ H$_{34}$ O$_2$) with 0.1 percent by volume of nanofluids is added into the Fe$_3$O$_4$ and DI water mixture. This dispersant drastically enhances the stability and increases the quality of dispersion process. The prepared fluid is shown in fig. 1 and it is found to be stable upto 35 days at atmospheric condition.
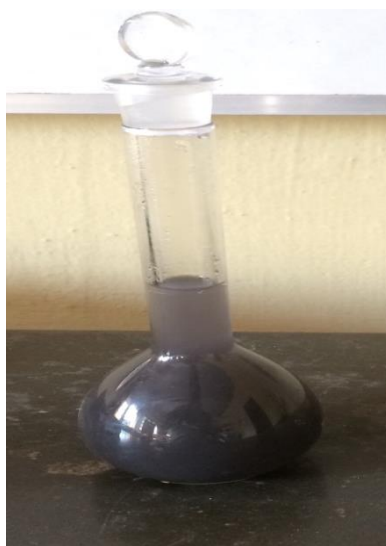

Figure 1: Prepared Fe$_3$O$_4$ water based Nanofluid

2.1.1.Fourier Transform infrared spectroscopy (FTIR)

In FTIR, IR radiation is passed through the sample. Some of the infrared radiation is adsorbed by the sample and some of it is passed through. The resulting spectrum represents the molecular adsorption and transmission.
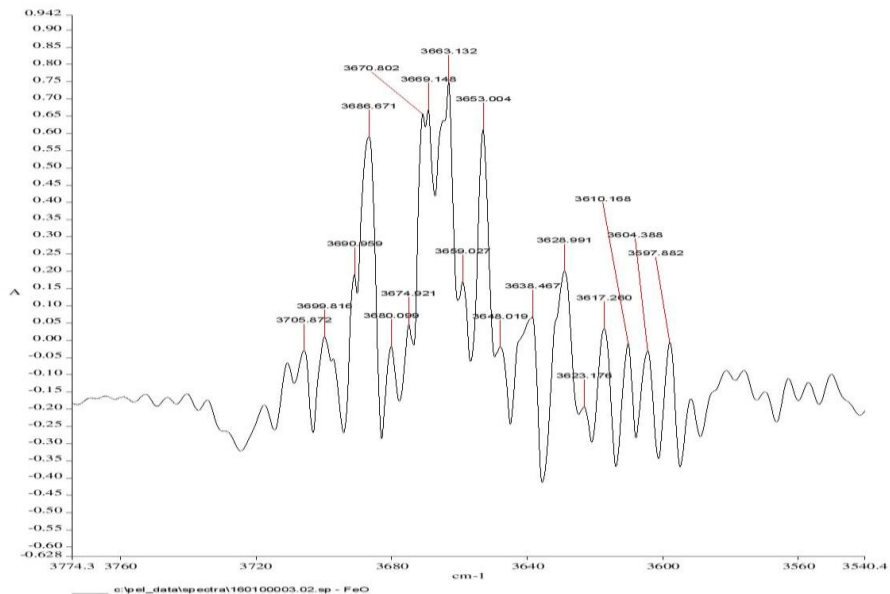

Figure 2: FTIR Spectra of Fe_3O_4 water based Nanofluid

From the fig 2. it is noted that the peak value becomes 3663.132 cm^{-1} that corresponds to a strong adsorption band of Fe-O stretching vibrations and the other one at 3705.872 cm^{-1} region is due to the O-H starching vibration of the $Fe_3 + O$. furthermore the FTIR spectrum shows an low adsorption band at approximately 3750 cm^{-1}, which shows the stretching vibration of the carboxyl group (C=O), associated to the Oleic acid molecule. Summarising, magnetite nanofluid have poly crystalline structure of converse spinal type and FTIR adsorption spectroscopy allowed identifying characterises features of the converse spinal type as well as a presence of certain types of chemical substances adsorbed on the surface of the nanofluids.

III.   MATERIALS AND METHODS

An experimental setup was built to carry out to compare the experimental RSM and CFD studies with 6063 AA Two-Phase Closed Thermosyphon (TPCT) container material along with Fe_3O_4 water based nano fluid working fluid. The photographic view of the experimental setup is shown in fig 3.

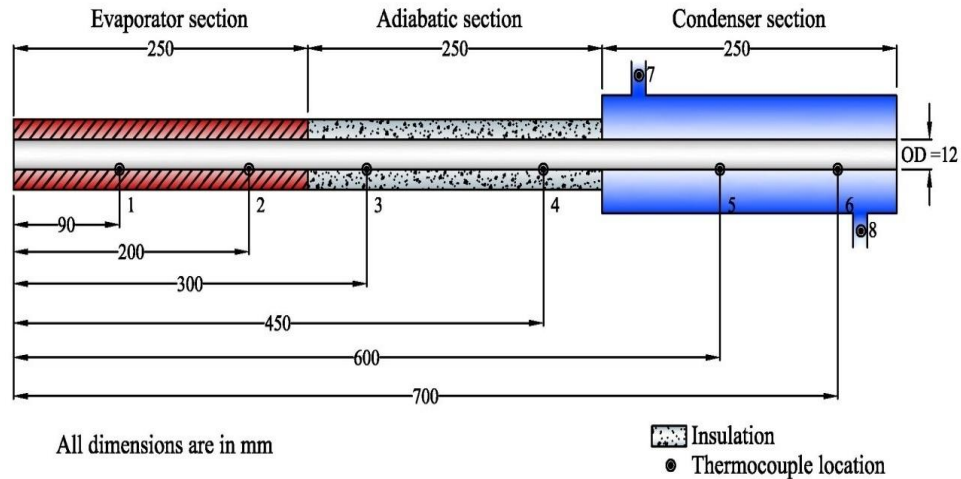**Figure 3:** Photographic View of Test Rig with 6063 AA TPCT

Figure 4: Constructional Details of 6063 AA TPCT

Fig 4 shows the constructional details of 6063 AA TPCT and the thermocouple location .The inclinometer (Bevel Protector) provision is made on the test rig to rotate the TPCT through 0° - 180° angle. The electrical heater of 200 watts capacity is wrapped around the evaporator section for supplying heat input. The three phases variac is used to regulate the power supply according to the need. The capacity of the variac which is used for this experiment is 1800 watts, 230 volts and 20 amps (III Phase). The wattmeter is used to determine the power supply in watts to the load given in the heater of the evaporator section through the three phase variac and its range is around 0-250 watts and 230 volts. The digital display in the wattmeter shows the value of load. The K-type thermocouples are soldered along the length of the TPCT at eight locations. All the eight K-type thermocouples are connected to the (countron, USB) data acquisition system for the better results in temperature measurement. The efficient way to measure the power output of TPCT by using the condenser jacket through which water is passed. In this experiment, the 6063 AA TPCT, a 6063 AA alloy jacket with an outer diameter of 30 mm, and length of 250 mm, having the inlet and outlet connections located diagonally across each other to induce swirl flow is designed.The mass flow rate of the coolant water from the water tank is controlled by rotometer.

1.1 Test Procedure

In order to validate the RSM model of the TPCT made of 6063AA with Fe_3O_4water based nano fluid as working fluid, BBD method was employed with three varying input parameters were used, namely heat input (A), angle of inclination (B) and flow rate of water in the condenser section (C) over the output response of thermal resistance (R_{th}) Table. 1 shows the process parameters and their levels. Table . 2 show the design of matrix.

Table 1: Process parameters and their levels

Parameters	Level		
	-1	**0**	**1**
Heat Input, W	90	120	150

Angle of inclination, °	30	60	90
Flow Rate, ml/min	100	150	200

Table 2: Design of Matrix

Std	Run	Factor 1 A: Heat input	Factor 2 B: angle	Factor 3 C: flow Rate
2	1	120	60	150
1	2	120	30	200
7	3	150	60	100
5	4	90	60	100
16	5	90	60	200
9	6	90	90	150
10	7	120	60	150
4	8	150	90	150
14	9	90	30	150
13	10	120	60	150
8	11	120	90	100
11	12	120	90	200
12	13	120	30	150
17	14	120	60	150
3	15	120	60	150
15	16	150	60	200
6	17	120	30	100

Design of Experiments (DOE) is an efficient procedure for planning experiments so that the data obtained can be analysed easily. The experimental task starts with selecting the input variables and the response (output) that is to be measured. 17 runs of simulation are arranged by three factors (BBD) as listed in table 2. First, the mass flow rate of pure water flowing through the condenser section is set using rotometer. The inclination angle of TCPT is fixed. The power supply is turned on and the heat input is increased with the help of variac. Approximately it took twenty minutes for 6063AA TPCT to attain the steady state. The temperature at each trial is recorded after the attainment of steady state condition using data acquisition system [USB-Countron].

3.2 FLUENT Modelling

A 6063 Aluminium Alloy (AA) TPCT with Fe3O4 water based nanofluid is modelled to account the heat transfer performance under the constant heat input, inclination angle and flow rate. The ANSYS FLUENT 12.0 software package is used to predict the temperature and the velocity magnitude profiles of the 6063 AA TPCT. The flow rate, the inclination angle and the heat input is maintained as 150W, 30° and 174.78 ml/min. Using VOF model and the Navier-Stokes equations the model has been validated. The VOF model and the Navier-Stokes equations for the VOF model are discussed below.

Continuity

$$\frac{\partial}{\partial t}(\rho) + \sum_{j=1}^{3} \frac{\partial}{\partial x_j}(\rho u_j) = S_M$$

Momentum

$$\frac{\partial}{\partial t}(\rho u_i) + \sum_{j=1}^{3} \frac{\partial}{\partial x_j}(\rho u_i u_j) = -\frac{\partial p}{\partial x_i} + \sum_{j=1}^{3} \frac{\partial}{\partial x_j}\left[\mu\left(\frac{\partial u_i}{\partial x_j} + \frac{\partial u_j}{\partial x_i} - \frac{2}{3}\delta_{ij}\sum_{i=1}^{3}\frac{\partial u_i}{\partial x_i}\right)\right] + S_{F,i}$$

Energy

$$\frac{\partial}{\partial t}(\rho E) + \sum_{j=1}^{3} \frac{\partial}{\partial x_j}(\rho E u_j) = \sum_{i=1}^{3}\sum_{j=1}^{3}\left(\frac{\partial}{\partial x_j}(\tau_{ij})u_i\right) - \sum_{j=1}^{3}\frac{\partial}{\partial x_j}q_j + S_E$$

In these equations, the density (ρ) and viscosity (μ) of the fluid depend on the volume fractions of each phase (α_k) and they are calculated by the following equations:

$$\rho = \sum_{k=1}^{2} \alpha_k \rho_k$$

$$\mu = \sum_{k=1}^{2} \alpha_k \mu_k$$

The VOF model treats energy (E) and temperature (T) as mass averaged variables:

$$E = \frac{\sum_{k=1}^{2} \alpha_k \rho_k E_k}{\sum_{k=1}^{2} \alpha_k \rho_k}$$

Where E_k for each phase is based on the specific heat of that phase and th shared temperature. The interface between two phases is tracked by the volume fraction. Conservation of α can be represented by the interface mass balance using the following equation:

$$\frac{\partial \alpha}{\partial t} + u.\nabla\alpha = 0$$

The 6063 AA TPCT with Fe3O4 water based nanofluid is created in ANSYS FLUENT 12.0. The constructional details, the properties of the material and the fluid are given in table 3.

Table 3: Constructional details and properties of the container material and nanofluid

S.No.	Construction	Values	Unit
1.	Total length of the pipe	750	Mm
2.	Evaporator section	250	Mm

3.	Adiabatic section	250	Mm
4.	Outer diameter of the pipe	12	Mm
5.	Inner diameter of the pipe	10	Mm
6.	Container material	6063 AA TPCT	
7.	Thermal conductivity of the material	200	W/mK
8.	Density of the material	2.7	g/cm^3
9.	Thermal expansion coefficient	23	µm/m˚C
10.	Thermal conductivity of Fe_3O_4 nanofluid	1.3032	W/mK
11.	Viscosity of Fe3O4 nanofluid	0.33	mPa·s
12.	Density of the fluid	1021.91	Kg/m^3
13.	Specific heat C_p	4154.89	j/kgK

3.2.1 Meshing

Meshing is carried out to represent a finite number of elements of the geometric structure. The presence of more ensures a higher accuracy. A 3D model of 6063 AA TPCT is created and meshing is carried out using ANSYS FLUENT 12.0. Free mesh is used in the entire region of the 6063 TPCT. The final grid consisted of 207393 nodes, 37, 40,500 faces and 7, 48,100 cells. A portion of the 6063 AA TPCT grid is shown in fig.5
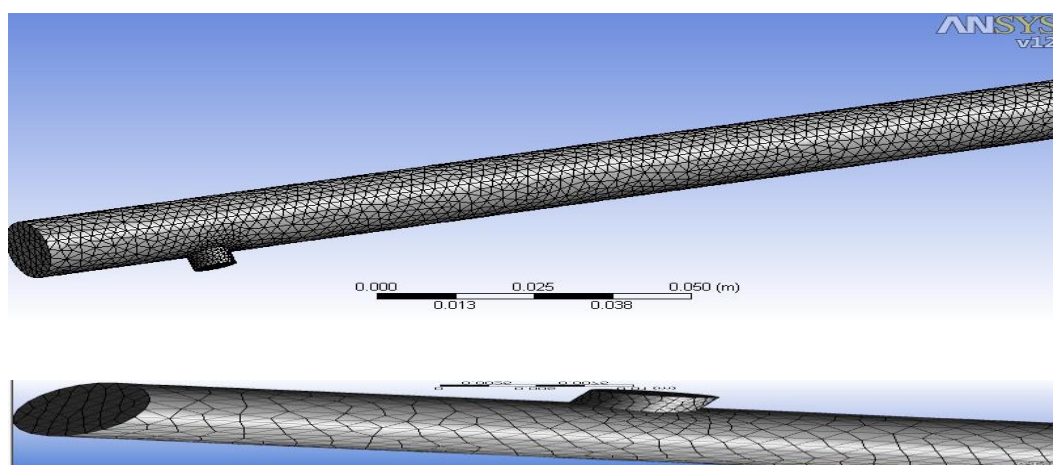

Figure 5: 3D mesh created on 6063 AA TPCT

3.2.1.1 Assumptions for the study

➢ Steady state conditions prevail

➢ Ambient losses are negligible

➢ The heat input, flow rate and inclination angle is maintained as constant

➢ The effects of the change of temperature at the entrance and exit of the TPCT are neglected.

Boundary conditions

➢ A non-slip boundary condition is imposed at the inner walls of the inner walls of the thermosyphon in order to simulate the heating and evaporation , a constant heat input is defined at the wall boundaries of the evaporator section.

➢ A zero heat input is defined as the boundary condition on the adiabatic section.

➢ The convective heat transfer coefficient was defined as the boundary on the overall sections of the TPCT.

3.3 Data reduction

Data reduction is the transformation of numerical or alphabetical digital information derived empirically or experimentally into a corrected, ordered, and simplified form. The basic concept is the reduction of multitudinous amounts of data down to the meaningful parts.

When information is derived from instrument readings there may also be a transformation from analog to digital form. When the data are already in digital form the 'reduction' of the data typically involves some editing, scaling, coding, sorting, collating, and producing tabular summaries. When the observations are discrete but the underlying phenomenon is continuous then smoothing and interpolation are often needed. Often the data reduction is undertaken in the presence of reading or measurement errors.

Thermal resistance is defined as the ratio of the temperature gradient between evaporator and condenser sections.

The thermal resistance of the thermosyphon (R_{th}) is evaluated by

$$R_{th} = \frac{T_{eavg} - T_{cavg}}{Q_{input}}$$

where, T_{eavg} and T_{cavg} are the arithmetic average of temperatures of the evaporator and the condenser sections respectively. The heating power input Q can be observed from wattmeter.

IV.   RESULT AND DISCUSSIONS

4.1 Effect of thermal resistance on various input parameters of 6063 AA TPCT with Fe_3O_4 water based nanofluid

The response considered was thermal resistance and the results are given below.

Table 4: ANOVA Table for thermal resistance (Response 1)

Response   1   RTH
ANOVA for Response Surface Quadratic Model
Analysis of variance table [Partial sum of squares - Type III]

Source	Sum of Squares	df	Mean Square	F Value	p-value Prob > F	
Model	0.006441	9	0.000716	64.11328	< 0.0001	Significant
A-HEAT INPUT	0.002269	1	0.002269	203.2609	< 0.0001	
B-ANGLE	5.08E-05	1	5.08E-05	4.550125	0.0703	
C-FLOW RATE	0.000109	1	0.000109	9.745749	0.0168	
AB	1.4E-05	1	1.4E-05	1.258333	0.2990	
AC	0.001034	1	0.001034	92.60259	< 0.0001	
BC	0.000708	1	0.000708	63.39054	< 0.0001	
A^2	1.64E-05	1	1.64E-05	1.470094	0.2647	
B^2	0.000102	1	0.000102	9.108858	0.0194	
C^2	0.001862	1	0.001862	166.81	< 0.0001	
Residual	7.81E-05	7	1.12E-05			
Lack of Fit	7.46E-05	3	2.49E-05	28.53418	0.1037	Not Significant
Pure Error	3.49E-06	4	8.72E-07			
Cor Total	0.006519	16				

The Model F-value of 64.11 implies the model is significant. There is only a 0.01% chance that a "Model F-Value" this large could occur due to noise. Values of "Prob > F" less than 0.0500 indicate model terms are significant. In this case A, C, AC, BC, B^2, C^2 are significant model terms. Values greater than 0.1000 indicate the model terms are not significant.

Final equation which is generated by DOE software 7.0 in terms of coded factors is given in equation 6.7

Final Equation in Terms of Coded Factors:

RTH $= +0.099 - 0.020 * A - 2.748E\text{-}003 * B - 3.688E\text{-}003 * C + 2.545E\text{-}003 * A * B - 0.016 * A * C + 0.013 * B * C + 2.218E\text{-}003 * A^2 - 5.114E\text{-}003 * B^2 + 0.022 * C^2$
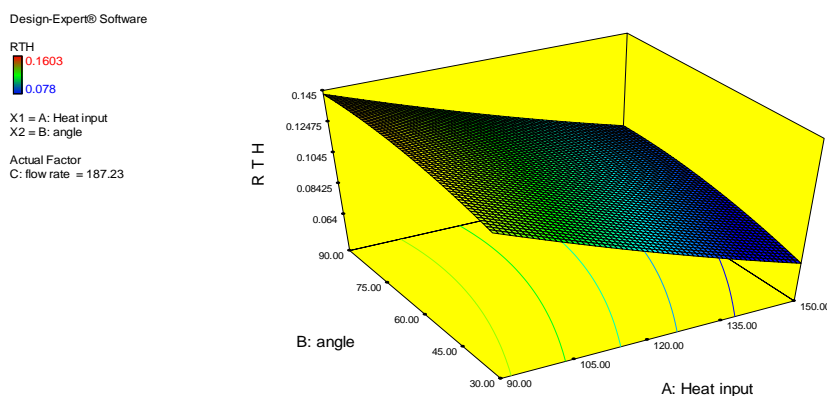

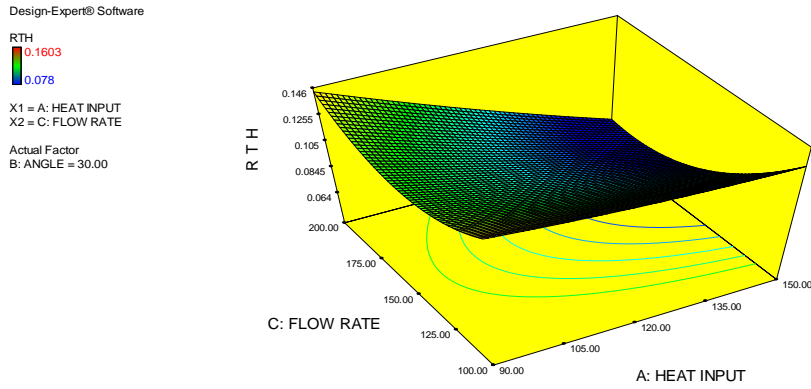**Figure 6:** RTH with respect to heat input and angle

Figure 7: RTH with respect to heat input and flow rate
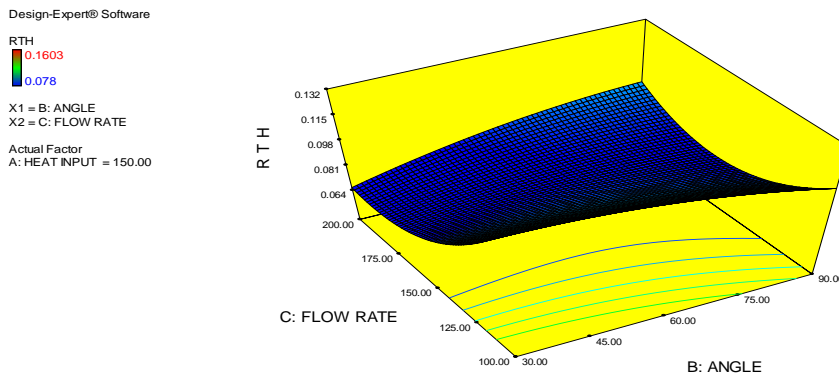

Figure 8: RTH with respect to flow rate and angle

The surface plot given in figure 6. shows the interactive effect of heat input and inclination angle on thermal resistance. It is found the increase in heat input, decreases the thermal resistance steeply to the minimum value of 0.064˚C/W. Increase in inclination angle with respect to thermal resistance shows a constant hike that occurs in the thermal resistance. From the fig 7.a steep reduction in thermal resistance has been observed with increase in heat input and flow rate which is of high range. On the other hand the minor increase in thermal resistance with the increase in heat input. Similarly increase in flow rate will also increase the thermal resistance. From the fig 8. is found that the factors angle and flow rate reduces the thermal resistance. The increase in angle of inclination pushes the thermal resistance evenly. The flow rate gradually increases the thermal resistance upto certain level and gets reduced. The combinational effect of these two factors is found to have a maximal decrease in thermal resistance as they both increase. From all the input parameters the value of thermal resistance is high at the higher inclination angle of 6063 AA TPCT; the maximum reduction of thermal resistance can be intensified by increasing the heat input and the flow rate. For this phenomenon two reasons can be considered (i) increase in heat input increases the wall temperature of the container material which enhances the thermal conductivity of the nanofluid from 0.876 to 1.303 W/mK(fig). (ii) the selected container material which is 6063 AA TPCT have a high thermal expansion coefficient and density, this will dramatically reduce the incipient boiling wall super heat of the 6063 AA surface and enhance the heat transfer. The experimental results of A.B.Solomon et al (2013) for anodised AL TPCT of length 350mm with an inner diameter of 16.5mm, tested with the heat input range of 50 to 250 Watts achieved a maximum reduction of thermal resistance in the higher heat input of 250W was observed as 0.1˚ C/W. In the present study the length of the 6063 AA TPCT is 750mm with an inner diameter of 10mm. It is tested with

the heat input range 90-150W. When compared with the above literature, it was found that the thermal resistance value achieved was 0.325°C/W whereas in the current study 0.064 was achieved at 150W. This may be due to the intensive property of the container material. Hence it can be considered that 6063 AA TPCT can be a good replacement for the anodised AL TPCT.

4.2. CFD Results and Discussion

The best value from the RSM model is simulated. The corresponding parameter is tabulated in table5.

Table 5: Input parameter for CFD simulation

Heat input	Angle	Flow rate
150	30°	174.78

Simulation for the chosen 6063 AA container material with Fe3O4water based nanofluid is performed by incorporating the heat input, the inclination angle and the flow rate condition proposed by the RSM. The axial temperatures along the TPCT are found out by simulation and are compared with the experimental results in order to validate the developed CFD models.
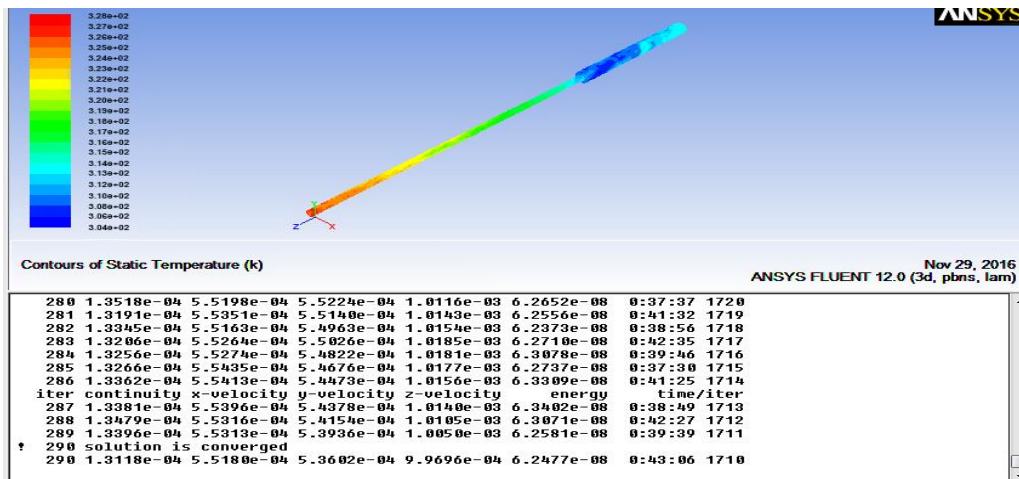

Figure 9: Contours of Static Temperature (k) for 6063 AA
TPCT with Fe_3O_4 Nanofluid

From the fig 9. it is seen that the temperature in the evaporator section is 328K (55°C) and leaves the condenser section 315K (42°C). The adiabatic section of the pipe having 322K, on the other hand the temperature leaves out from the evaporator is 324K and the inlet of the condenser section at 304K (31°C).

V.   CONCLUSION

On the whole the nanofluids are applied in heat transfer due to their potential in enhancing the thermal performance of thermosyphon. The result in the present study for 6063 AA TPCT filled with Fe3O4 nanofluid is compared with the CFD model in the following table.6.

Table 6: Comparison parameters for experimental and CFD model over thermal resistance

Parameters	Experimental	CFD
Thermal Resistance, R_{th}, ˚C/W	0.066	0.0733

Since the percentage of deviation in experimental and CFD is 9.95%, therefore the model is accepted.

REFERENCE

1. Faghri, A. (1995). Heat pipe science and technology. Global Digital Press.

2. Manohar, M., Joseph, J., Selvaraj, T., & Sivakumar, D. (2013). Application of Box Behnken design to optimize the parameters for turning Inconel 718 using coated carbide tools. International Journal of Scientific & Engineering Research, 4(4): 620-644.

3. Perincek, O., & Colak, M. (2013). Use of Experimental Box-Behnken Design for the Estimation of Interactions Between Harmonic Currents Produced by Single Phase Loads. Interactions, 3(2).

4. Krishna, D., & Siva Krishna, K. (2013). Removal of chromium from aqueous solution by borasus flabellifer coir powder as adsorbent. Elixir: Chemical Engineering, 56: 13308-1331.

5. Fadhl, Bandar, Luiz C. Wrobel, and Hussam Jouhara. (2013). Numerical modelling of the temperature distribution in a two-phase closed thermosyphon. Applied Thermal Engineering. 60.1: 122-131

6. Xu, Zhi, et al. (2016). Modeling the phase change process for a two-phase closed thermosyphon by considering transient mass transfer time relaxation parameter. International Journal of Heat and Mass Transfer. 101: 614-619.

7. Schwertmann, U., & Cornell, R.M. (2008). Iron oxides in the laboratory: preparation and characterization. John Wiley & Sons

8. Cordova, G., Attwood, S., Gaikwad, R., Gu, F., & Leonenko, Z. (2014). Magnetic Force Microscopy Characterization of Superparamagnetic Iron Oxide Nanoparticles (SPIONs). Nano Biomed. Eng, 6(1): 31-39.

9. Huminic, G., Huminic, A., Morjan, I., & Dumitrache, F. (2011). Experimental study of the thermal performance of thermosyphon heat pipe using iron oxide nanoparticles. International Journal of Heat and Mass Transfer, 54(1): 656-661.

10. Xie, J., & Jon, S. (2012). Magnetic nanoparticle-based thermostics. Theramostics, 2(1), 122-124.

11. Tae-Keun, H., & Ho-Soon, Y. (2005). Nanoparticle-dispersion-dependent thermal conductivity in nanofluids. Journal of Korean Physical Society, 47: 321.

12. Goshayeshi, H.R., Safaei, M. R., Goodarzi, M., & Dahari, M. (2016). Particle size and type effects on heat transfer enhancement of Ferro-nanofluids in a pulsating heat pipe. Powder Technology, 301: 1218-1226.

13. Solomon, A.B., Mathew, A., Ramachandran, K., Pillai, B.C., & Karthikeyan, V.K. (2013). Thermal performance of anodized two phase closed thermosyphon (TPCT). Experimental Thermal and Fluid Science, 48: 49-57.